Atmos. Chem. Phys., 22, 16123–16135, 2022
https://doi.org/10.5194/acp-22-16123-2022

Atmospheric Chemistry and Physics
Open Access
EGU

Research article

Reconsideration of surface tension and phase state effects on cloud condensation nuclei activity based on the atomic force microscopy measurement

Chun Xiong[1], Xueyan Chen[3], Xiaolei Ding[4], Binyu Kuang[1], Xiangyu Pei[1], Zhengning Xu[1], Shikuan Yang[3], Huan Hu[4], and Zhibin Wang[1,2,5]

[1]College of Environmental and Resource Sciences, Zhejiang Provincial Key Laboratory of Organic Pollution Process and Control, Zhejiang University, Hangzhou 310058, China
[2]Hangzhou Global Scientific and Technological Innovation Center, Hangzhou 311200, China
[3]Institute for Composites Science Innovation, School of Materials Science and Engineering, Zhejiang University, Hangzhou 310027, China
[4]Zhejiang University-University of Illinois at Urbana-Champaign Institute, International Campus, Zhejiang University, Haining 314400, China
[5]Key Laboratory of Environment Remediation and Ecological Health, Ministry of Education, Zhejiang University, Hangzhou 310058, China

Correspondence: Zhibin Wang (wangzhibin@zju.edu.cn) and Huan Hu (huanhu@intl.zju.edu.cn)

Received: 13 September 2022 – Discussion started: 16 September 2022
Revised: 6 December 2022 – Accepted: 8 December 2022 – Published: 23 December 2022

Abstract. Dicarboxylic acids are ubiquitous in atmospheric aerosol particles, but their roles as surfactants in cloud condensation nuclei (CCN) activity remain unclear. In this study, we investigated CCN activity of inorganic salt (sodium chloride and ammonium sulfate) and dicarboxylic acid (including malonic acid (MA), phenylmalonic acid (PhMA), succinic acid (SA), phenylsuccinic acid (PhSA), adipic acid (AA), pimelic acid (PA), and octanedioic acid (OA)), mixed particles with varied organic volume fractions (OVFs), and then directly determined their surface tension and phase state at high relative humidity (over 99.5 %) via atomic force microscopy (AFM). Our results show that CCN-derived κ_{CCN} of studied dicarboxylic acids ranged from 0.003 to 0.240. A linearly positive correlation between κ_{CCN} and solubility was obtained for slightly dissolved species, while negative correlation was found between κ_{CCN} and molecular volume for highly soluble species. For most inorganic salts and dicarboxylic acids (MA, PhMA, SA, PhSA and PA), a good closure within 30 % relative bias between κ_{CCN} and chemistry-derived κ_{Chem} was obtained. However, κ_{CCN} values of inorganic salt–AA and inorganic salt–OA systems were surprisingly 0.3–3.0 times higher than κ_{Chem}, which was attributed to surface tension reduction, as AFM results showed that their surface tensions were 20 %–42 % lower than that of water (72 mN m^{-1}). Meanwhile, semisolid phase states were obtained for inorganic salt–AA and inorganic salt–OA and also affected hygroscopicity closure results. Our study highlights that surface tension reduction should be considered when investigating aerosol–cloud interactions.

Published by Copernicus Publications on behalf of the European Geosciences Union.

1 Introduction

Atmospheric particles can indirectly affect global climate through their impacts on aerosol–cloud interaction by serving as cloud condensation nuclei (CCN; Rosenfeld et al., 2014). Exploring the factors affecting CCN activation can help us to understand the aerosol–cloud interactions and thus decrease the uncertainty in the assessment of climate model. Köhler theory provides the basis for linking CCN activity with aerosol thermodynamic properties (Köhler, 1936), in which size and chemical composition are key factors to determine the activation of aerosol particles. Previous studies pointed out that aerosol number size distribution was essential to determine CCN concentration in addition to composition (Dusek et al., 2006; Gunthe et al., 2009; Rose et al., 2010). The role of particle chemistry in the activation process, however, is still debatable due to the complexity of chemical constitution (Bhattu and Tripathi, 2015; Noziere, 2016).

Single-parameter κ was introduced in Köhler theory to describe hygroscopicity of aerosol particles (Petters and Kreidenweis, 2007). κ-Köhler theory usually performed well in predictions of hygroscopicity and CCN number concentration (Rose et al., 2010; Kawana et al., 2016; Cai et al., 2020; Zhang et al., 2020). However, a remarkable offset was also found because of the simplifications in κ-Köhler theory (Ruehl et al., 2016; Ovadnevaite et al., 2017). For example, an aerosol droplet is assumed to be diluted near activation, and surface tension is usually simply treated as that of pure water, which is sometimes not reasonable in the presence of atmospheric surfactants (Lowe et al., 2019). Many previous studies investigated the surface tension effect of atmospheric surfactants on aerosol CCN activity (Ruehl and Wilson, 2014; Ruehl et al., 2016; Ovadnevaite et al., 2017). At Mace Head, Ovadnevaite et al. (2017) observed significant underestimation of CCN number concentration (one-tenth) in a nascent ultrafine-mode event with high organic mass fraction (55 %). The underestimation was improved by applying lower water surface tension ($\sim$ 68 % of water surface tension). For surfactant sodium octyl sulfate, Peng et al. (2022) found that CCN-derived κ_{CCN} was around 2.4 times larger than the growth-factor-derived κ_{GF}, which was ascribed to the surface tension reduction and solubility limit. Though established thermodynamic models considering surface tension reductions such as the compressed film model (Ruehl et al., 2016) and liquid–liquid-phase separation model (Ovadnevaite et al., 2017; Liu et al., 2018) explained the discrepancies in CCN activity or CCN number concentration closure, datasets with direct measurements of surface tension for sub-micrometer particles are very rare.

Dicarboxylic acids are ubiquitous in atmospheric aerosol particles as a main contributor to organic aerosol mass (mass contribution to total particulate carbon exceeds 10 % in remote area) (Römpp et al., 2006; Ho et al., 2010; Hyder et al., 2012). Primary emission (e.g., biomass burning and fossil fuel combustion) and secondary formation (e.g., photooxidation of unsaturated fatty acids) were major sources of dicarboxylic acids (Ho et al., 2010). Furthermore, dicarboxylic acids are also known as important atmospheric surfactants, and their surface activities in water solutions showed a positive relation with carbon number (Aumann et al., 2010). Currently, most studies investigated the surface tension effect of dicarboxylic acids on CCN activation by measuring surface tension of their solutions and using models based on solution results (Lee and Hildemann, 2013, 2014; Ruehl et al., 2016; Zhang et al., 2021; Vepsäläinen et al., 2022). However, the values derived from bulk solutions may not be a reasonable representation for aerosol particles because their high surface-to-volume ratio may affect the distribution of surfactant between surface and bulk (Ruehl et al., 2010; Ruehl and Wilson, 2014). Recently, new methods of surface tension measurement for particles were introduced such as micro-fluid (Metcalf et al., 2016) and optical tweezers (Bzdek et al., 2020), but their samples were micrometer-sized droplets. Morris et al. (2015) presented a way to directly measure surface tension of sub-micrometer particles under controlled relative humidity (RH) by atomic force microscopy (AFM). Later, AFM was further reported to be an important tool to probe the phase state of individual particles (Lee et al., 2017a, b; Lee and Tivanski, 2021). However, most measurements using AFM were performed with RH under 95 % (Morris et al., 2015; Lee et al., 2017b; Ray et al., 2019; Lee et al., 2020) but rarely in higher RH conditions. When RH approaches 100 %, the Kelvin effect becomes comparable to the Raoult effect in controlling hygroscopicity, and thus measurements around 100 % RH can help resolve discrepancies between sub-saturated hygroscopicity and CCN activity (Ruehl and Wilson, 2014).

In this study, we first measured CCN activities of internal mixtures containing inorganic salt and dicarboxylic acid. Following this, we directly obtained their surface tension and phase states by AFM under relatively high RH (over 99.5 %). Our results could provide a direct dataset of the surface tension and phase state of internally mixed particles of inorganic salts and dicarboxylic acids, which would help to decrease the uncertainty for climate models.

2 Methods

2.1 Experiments

2.1.1 Chemicals

The nine compounds used in the present study were sodium chloride (NaCl), ammonium sulfate (AS), malonic acid (MA), phenylmalonic acid (PhMA), succinic acid (SA), phenylsuccinic acid (PhSA), adipic acid (AA), pimelic acid (PA), and octanedioic acid (OA). The relevant properties investigated in this study are summarized in Table 1.

Table 1. Substances and their relevant properties investigated in this study.

Compounds	Molar weight ($g\,mol^{-1}$)	Density ($g\,cm^{-3}$)	Solubility ($g\,L^{-1}$)	DRH (% RH)	Purity	Supplier
NaCl	58.44[a]	2.16[a]	360[b]	73–77[c]	≥ 99.8 %	Sinopharm chemical reagent
AS	132.13[a]	1.77[a]	770[b]	78–82[c]	≥ 99 %	Sigma Aldrich
MA	104.06[a]	1.63[a]	1400[b]	65–76[c]	≥ 99 %	Sigma Aldrich
PhMA	180.16[a]	1.40[a]	131[a]	NA[f]	98 %	Aladdin
SA	118.09[a]	1.57[a]	80[b]	98[d]	≥ 99 %	Aladdin
PhSA	194.19[a]	1.13[a]	241[a]	NA[f]	98 %	Macklin
AA	146.14[a]	1.36[a]	14.4[b]	∼ 100[e]	≥ 99.8 %	Sinopharm chemical reagent
PA	160.17[a]	1.28[a]	25[b]	> 90[c]	99 %	Macklin
OA	174.20[a]	1.16[a]	12[a]	> 90[c]	99 %	Aladdin

[a] https://comptox.epa.gov/ (last access: 3 August 2022). [b] https://www.chemicalbook.com/ (last access: 3 August 2022). [c] Peng et al. (2022) and references therein. [d] Peng et al. (2001). [e] Parsons et al. (2004). DRH stands for deliquescence relative humidity. [f] NA indicates that no reported results are available.

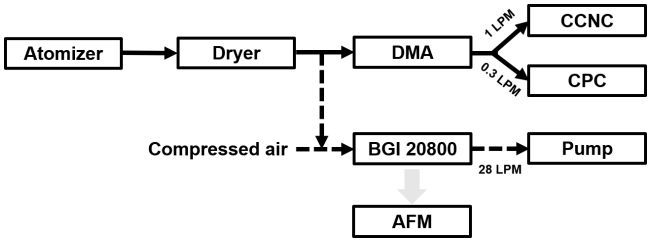

Figure 1. Schematic illustration of the instrumental setup. The arrow indicates the flow direction. LPM stands for liters per minute.

2.1.2 CCN activity measurements

The measurement setup is shown in Fig. 1. In brief, particles containing single and mixed chemicals were generated by clean and particle-free compressed air with water solutions (∼ 1 ‰) by a constant output atomizer (TSI 3079A). The solutions were prepared by using ultrapure water (Millipore, resistivity ≤ 18.2 MΩ). After drying (RH < 15 %), monodispersed aerosol particles were obtained by differential mobility analyzer (DMA, TSI 3081) with a sheath to sample flow ratio of 10, and they then were split between a condensation particle counter (CPC, TSI 3772) for measuring number concentration of total particles (N_{CN}) and a cloud condensation nuclei counter (CCNC, DMT-200) for measuring the number concentration of CCN (N_{CCN}).

In this study, the CCNC was operated in scanning flow CCN analysis (SFCA) mode, which has been introduced and explained elsewhere (Moore and Nenes, 2009). In short, the pressure and ΔT of CCNC were kept constant, the flow rate was continuously and linearly varied from 0.2 to 1 L min^{-1} or vice versa (1–0.2 L min^{-1}) within 125 s, and the interval time for stabilization was 25 s. The supersaturations in CCNC were calibrated under four ΔT values (4, 6, 10 and 18 K). We obtained sigmoidal curves of activation ratio (N_{CCN}/N_{CN}) versus flow rate and fitted the inflection point of the curves as the critical flow rate Q_{50}. Ammonium sulfate was used to determine supersaturation ratio with an activity parameterization Köhler model AP3, as suggested by Rose et al. (2008). The calibration results are shown in Fig. S1 in the Supplement.

2.1.3 Surface tension measurements

As shown in Fig. 1, samples for AFM analysis were collected through deposition by impaction with an eight-stage nonviable particle sizing sampler (BGI20800, BGI) onto hydrophobic silicon wafers. The hydrophobic silicon wafers have a polydimethylsiloxane brush surface, and thus solute can be collected into the solute aggregate on the surface after water evaporation when RH varies (especially when RH decreases; Ding et al., 2020). The aerodynamic size of collected particles ranged from 0.4 to 1 µm (50 % efficiency). The deposited substrate particles were stored under dry conditions (RH < 10 %), and most of the samples were studied on the same day to avoid possible sample aging.

Surface tension measurement was performed using an AFM system (Cypher ES, Asylum Research). Cypher ES contains a small cell with an air inlet and outlet, which enables us to scan samples under different environmental conditions (such as RH). RH in a cell was achieved and maintained by humidified flow. RH in a cell was measured by an RH sensor (SHT 85, ±1.5 % uncertainty, Sensirion Inc.). Custom-built high aspect ratio (HAR) platinum AFM probes with a constant diameter and a nominal spring constant of ∼ 3.0 N m^{-1} were used for particle imaging and surface tension measurements (Fig. S2; Morris et al., 2015). The platinum nanoneedles could measure surface tension of pure water and 1,3-propanediol (Fig. S3) well. The procedures of making nanotips were described in detail in Ding et al. (2022), and thus only a brief description will be given here. First, a dual beam focused ion beam (FIB, ZEISS crossbeam 350) microscope was used to etch the top of the tip

(Multi75Al-G purchased from BudgetSensors Inc.), making the etched tip flat. Following this, the FIB was used to deposit a cylindrical metal platinum column (100–500 nm diameter) onto the flat surface of the etched tip.

The principles of surface tension measurement using AFM have already been described elsewhere (Yazdanpanah et al., 2008; Morris et al., 2015; Lee et al., 2017a). Collected samples were first imaged in tapping mode to locate individual particles under dry condition (RH < 10 %), then the RH gradually was increased to over 99.5 % over ∼ 40 min (Fig. S4). Force–distance plots of droplets were obtained by contact mode. A tip velocity of 1–2 µm s^{-1} and dwell time of 1–2 s were used for all measurements (Kaluarachchi et al., 2021). More than 10 force plots were collected on at least five individual droplets in order to decrease uncertainties (e.g., sensor accuracy). The precise diameter of the nanoneedle was calibrated by measuring the surface tension of pure water by adding a water droplet (2–3 mm height) onto a silicon wafer (Kaluarachchi et al., 2021). A new probe was used for different chemicals in order to avoid possible contamination of the AFM probe. However, it should be noted that the potential uncertainty introduced due to the different particle diameter in CCN activity (ranging from 50 to 260 nm) and AFM experiments (0.4–1 µm) is not taken into account because the size dependence of surface tension is not significant unless the solution droplets are smaller (down to 6 nm; Cheng et al., 2015).

2.2 Theory

Based on κ-Köhler theory, the hygroscopicity parameter κ_{CCN} for individual pure components and mixed aerosols can be calculated by

$$\kappa_{CCN} = \frac{4A^3}{27 D_d^3 \ln^2(1+s_c)}, A = \frac{4 M_w \sigma_w}{RT\rho_w}, \quad (1)$$

where σ_w, M_w, and ρ_w are surface tension, molecular weight, and density of water, respectively. R is the universal gas constant, and T is temperature (298.15 K). s_c is critical supersaturation ratio. D_d is dry diameter. In addition, the hygroscopicity κ of the multicomponent chemical system can also be calculated assuming a Zdanovskii–Stokes–Robinson (ZSR) simple mixing rule. κ based on the chemical composition (κ_{Chem}) of mixed aerosol was calculated by

$$\kappa_{Chem} = OVF \times \kappa_{org,CCN} + (1 - OVF) \times \kappa_{inorg,CCN}, \quad (2)$$

where $\kappa_{org,CCN}$ and $\kappa_{inorg,CCN}$ are obtained κ_{CCN} values of single organic acid and inorganic salt. OVF indicates the organic volume fraction of mixed particles.

As described by Morris et al. (2015), the basis of surface tension measurement for a liquid droplet by AFM was calculated by

$$\sigma = \frac{F_r}{2\pi r}, \quad (3)$$

where F_r is the retention force to break the meniscus using the tip of the AFM probe, r is the radius of the AFM probe tip, and σ is surface tension of the droplet. The retention force is the force difference before and after the probe was just retracted from the droplet.

3 Results and discussion

3.1 κ_{CCN} of a single component

κ_{CCN} values for single-component aerosols were summarized in Table 2. κ_{CCN} of NaCl, AS, MA, SA, and AA were 1.325 ± 0.038, 0.562 ± 0.059, 0.240 ± 0.036, 0.204 ± 0.023, and 0.008 ± 0.001, respectively, being overall consistent with previous results (Petters and Kreidenweis, 2007; Kuwata et al., 2013). κ_{CCN} of NaCl and MA were slightly higher and AS was slightly lower than those reported in Petters and Kreidenweis (2007). This may be ascribed to the solute purity (Hings et al., 2008). Based on the same reason, κ_{CCN} of PA (0.112 ± 0.010) and OA (0.003 ± 0.0002) values were 20 % lower and twice as high, respectively, compared to those reported by Kuwata et al. (2013). κ_{CCN} values of PhMA and PhSA were 0.183 ± 0.032 and 0.145 ± 0.017, respectively, which to our knowledge is the first time that they have been reported.

Solubility and molar volume of dicarboxylic acids were essential factors influencing their hygroscopicity (Pradeep Kumar et al., 2003; Han et al., 2022). Therefore, a solubility criterion of 100 g L^{-1} was used in our study to distinguish the effect of solubility of highly soluble (with water solubility over 100 g L^{-1}) and slightly soluble organics (with water solubility below 100 g L^{-1}) on their hygroscopicity, according to Kuwata et al. (2013) and Luo et al. (2020). As shown in Fig. 2a, the κ_{CCN} values for highly soluble components decreased linearly with increased molecular volumes. This trend was similar to κ_{CCN} values for sugar and dicarboxylic acids reported by Chan et al. (2008). In Fig. 2b, κ_{CCN} values of barely soluble components (AA, PA, SA, and OA) showed an increased trend with solubility, as organic matter with higher water solubility would dissolve more and have a higher molar concentration, resulting in a reduction in water activity and higher hygroscopicity (Luo et al., 2020; Han et al., 2022).

Organic functional groups could also affect hygroscopicity (Suda et al., 2014; Petters et al., 2017). κ_{CCN} of PA (0.112) was higher than that of AA (0.008) and OA (0.003), which is contrary to results in Suda et al. (2014) and Petters et al. (2017), where hygroscopicity decreased with increased number of methylene. This phenomenon was attributed to the odd–even effect of dicarboxylic acids, that is, diacids with odd numbers of carbon atoms being more soluble than those with adjacent even numbers (Zhang et al., 2013). Furthermore, κ_{CCN} values of PhMA and PhSA were both lower than those of MA and SA, respectively, indicating that the addition of phenyl showed negative effects on hygroscopic-

Table 2. Summary of κ_{CCN} for single-component particles.

Chemicals	D_d (nm)	κ_{CCN} mean ± standard deviation	Previous reported κ_{CCN}
NaCl	50, 65, 76, 88, 100	1.325 ± 0.038	1.28[a]
AS	50, 65, 76, 88, 100	0.562 ± 0.059	0.61[a]
MA	50, 65, 76, 88, 100	0.240 ± 0.036	0.227[a]
PhMA	50, 65, 76, 88, 100	0.183 ± 0.032	NA[c]
SA	50, 65, 76, 88, 100	0.204 ± 0.023	0.166–0.295[a]
PhSA	50, 65, 76, 88, 100	0.145 ± 0.017	NA[c]
AA	140, 160, 180, 200	0.008 ± 0.001	0.005–0.008[b]
PA	65, 76, 88, 100	0.112 ± 0.010	0.14[b]
OA	200, 220, 240, 260	0.003 ± 0.0002	0.001[b]

[a] Petters et al. (2007). [b] Kuwata et al. (2013) and references therein. [c] NA indicates that no reported results are available.

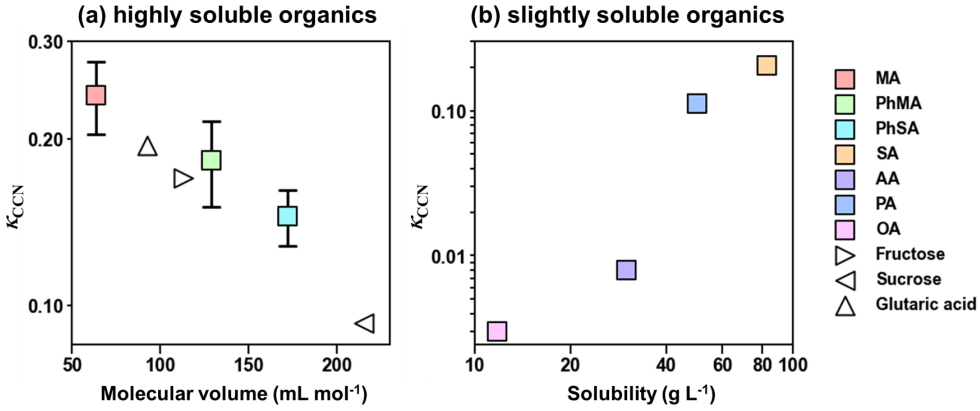

Figure 2. κ_{CCN} of organic compounds as a function of **(a)** molecular volume and **(b)** solubility. Solid squares represent κ_{CCN} results in this study, while hollow triangles are κ_{CCN} results obtained from Chan et al. (2008).

ity. The addition of a phenyl substitution increased the molar volumes of MA and SA and may contribute to the drops in hygroscopicity (Petters et al., 2009).

3.2 κ_{CCN} of mixed inorganic salt and dicarboxylic acid components

Figure 3 presents the κ_{CCN} values of mixed inorganic salt and dicarboxylic acid particles with varied organic volume fractions (OVF). Overall, κ_{CCN} of each inorganic salt and dicarboxylic acid system showed a decreased trend with increased OVF. For example, κ_{CCN} of AS and MA particles with OVF of 57 %, 73 %, and 88 % were 0.399, 0.373, and 0.336, respectively. Larger fractions of dicarboxylic acids (with low hygroscopicity compared to inorganic salts) caused greater decreases in hygroscopicity in inorganic salt and dicarboxylic acid systems. As for inorganic salt and dicarboxylic acid systems with the same OVF, κ_{CCN} values of systems of AS–MA, AS–SA, AS–PhMA, AS–PhSA, and AS–PA with 57 % OVF were 0.399, 0.382, 0.364, 0.340, and 0.334, respectively, following the order of κ_{CCN} values for single dicarboxylic acid (Fig. 3a). However, κ_{CCN} values of NaCl–AA and NaCl–OA mixed particles with OVF of 60 % were 0.734 and 0.685, even higher than that of NaCl–MA (0.639), demonstrating an opposite trend with respect to those of single components. This discrepancy could be ascribed to surface tension reduction because AA and OA showed different physical properties (e.g., deliquescence point, surface activity and solubility) when compared with the other organics and thus may result in distinct microphysics processes during interactions with inorganic salts and water content. AA and OA have the lowest solubilities and highest deliquescence RHs (Table 1) among experimental dicarboxylic acids, which potentially led to their weak CCN activity (Hings et al., 2008). However, inorganic salts were found to facilitate the deliquescence of dicarboxylic acid (Bilde and Svenningsson, 2004; Sjogren et al., 2007; Minambres et al., 2013). Mixed AS–AA particles deliquescence under 78 %–83 % RH with mass fractions of AA between 50 %–80 % (Sjogren et al., 2007). Small amount of NaCl (2 % mass faction) could notably decrease s_c of AA with 80 nm dry diameter from over 2 % to ∼ 0.6 % (Bilde and Svenningsson, 2004). Thus, addition of inorganic salts facil-

itates deliquescence of OA and AA under lower RH, further promotes their phase state transition from solid to liquid (or semisolid), and reduces their surface tension. Based on surface tension results of water solutions, Aumann et al. (2010) reported that surface activities of dicarboxylic acids were increased with their carbon number. Therefore, surface tensions of inorganic salt–AA and inorganic salt–OA systems may decrease more than the rest of the acid-containing particles, resulting in their relatively high κ_{CCN}. This indication was further confirmed by AFM surface tension measurement, as discussed in Sect. 3.4.

3.3 Closure study between κ_{CCN} and κ_{Chem}

κ_{CCN} and κ_{Chem} values for inorganic mixed salt and dicarboxylic acid particles are shown in Fig. 4. κ_{CCN} values of mixed particles including inorganic salt and most dicarboxylic acids (MA, PhMA, SA, PhSA, and PA) could be predicted using the ZSR mixing rule with a relative difference below 30 % (Fig. 4a). Similar results have been found in previous lab and field studies (Ruehl et al., 2012; Kuwata et al., 2013; Wu et al., 2013; Dawson et al., 2016; Nguyen et al., 2017; Ovadnevaite et al., 2017), indicating that a semi-experimental ZSR mixing rule could be a useful method to predict mixed-particle hygroscopicity and CCN activation. For instance, Dawson et al. (2016) reported consistency between κ_{CCN} and κ_{Chem} for NaCl xanthan gum and mixed $CaCO_3$ and xanthan gum particles within 10 % uncertainty. Wu et al. (2013) also obtained the same closure results in a field study in central Germany for particles containing 60 %–80 % organic mass fraction and 30 %–50 % inorganic salts. Meanwhile, CCN studies also found that using κ_{Chem} could predict measured CCN number concentration well (Juranyi et al., 2010; Rose et al., 2010; Almeida et al., 2014; Kawana et al., 2016; Cai et al., 2020; Zhang et al., 2020). However, for inorganic–AA and inorganic–OA mixed particles (Fig. 4b), their κ_{CCN} values were 0.3–3.0 times higher than κ_{Chem}. As discussed in Sect. 3.2, surface tension reduction was one of the potential causes leading OA and AA with strong surface activity and low solubilities to result in stronger surface tension reduction than most of the other dicarboxylic acids. In addition, the underprediction showed a gradual increasing trend with increased OVF since increased OVF led to a higher concentration of organics, thus leading to more surface tension reduction. Surface tension reduction in water solutions caused by atmospheric surfactants were observed frequently in previous studies (Facchini et al., 1999; Gerard et al., 2016). Results have shown that neglecting surface tension reduction may lead to higher κ_{CCN} values than κ_{Chem} or growth-factor-derived κ_{GF} (Irwin et al., 2010; Wu et al., 2013; Zhao et al., 2016; Hu et al., 2020; Peng et al., 2021), as well as underpredictions of CCN number concentration (Good et al., 2010; Asa-Awuku et al., 2011; Ovadnevaite et al., 2017; Cai et al., 2020). Hu et al. (2020) reported that κ_{Chem} underpredicted κ_{CCN} by 13 % and 18 % at supersaturation ratios of 0.1 % and 0.3 %, respectively, which may be attributed to the depression of droplet surface tension by potential surface-active organics. Likewise, Ovadnevaite et al. (2017) only predicted one-tenth of the measured CCN number concentration in a nascent ultrafine-mode event because of the surface tension reduction, and this notable underestimation was improved by applying lower water surface tension ($\sim$ 68 % of water surface tension) in κ-Köhler theory.

Apart from surface tension reduction, aerosol phase states could also bring uncertainty to critical supersaturation and hygroscopicity predictions (Henning et al., 2005; Hodas et al., 2015; Peng et al., 2016; Zhao et al., 2016). Being different from a traditional Köhler curve as they only one maximum, modified Köhler curves for mixed inorganic salt and slightly soluble dicarboxylic acid (e.g., AA) particles that account for limited solubility obtained two maxima in their critical supersaturation ratios, and the higher value among the two maxima determined the CCN activation (Bilde and Svenningsson, 2004). The maximum at the larger wet diameter is identical to that obtained by assuming that the organic acids are infinitely soluble in water (i.e., classical Köhler theory). The other maximum with a smaller wet diameter represents the point that all slightly soluble material is fully dissolved and it can also be viewed as an activation barrier due to the presence of an undissolved solid component of organic acid (Henning et al., 2005). Pajunoja et al. (2015) reported that biogenic secondary organic aerosol (SOA) particles formed from isoprene showed an increased trend in their hygroscopicity parameter from 0.05 to nearly 0.15 when RH increased from 40 % to supersaturation. They indirectly found the biogenic SOA to be semisolid phase; thus, the increased trend of hygroscopicity κ was explained by the gradual phase transition from solid to semisolid (or liquid) with raised RH because water content may gradually wet and dissolve the organic surface and form a water film (Pajunoja et al., 2015). The phase transition (or water film formation) of pure OA and AA would be difficult (i.e., high RH is required) because of their high deliquescence point and low solubilities but could be made easier (i.e., required high RH is decreased) via the addition of inorganic salts. Overall, the phase state and surface tension of atmospheric aerosol were two essential factors influencing their hygroscopicity and CCN activation. Though there are several indirect ways of detecting aerosol phase state (Pajunoja et al., 2015; Shiraiwa et al., 2017), current studies of direct measurements are still very limited.

3.4 Phase state and surface tension of mixed inorganic salt–dicarboxylic acid particles

3.4.1 Phase state

We obtained phase states of inorganic salt and dicarboxylic acid under high RH (over 99.5 %) by analyzing the shapes of force plots based on the AFM system (Lee et al., 2017a; Lee

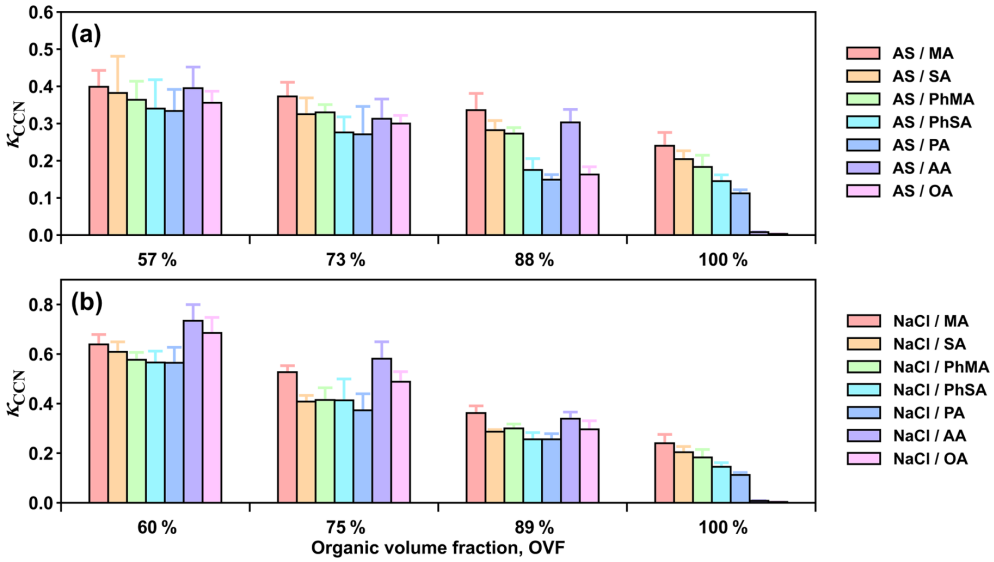

Figure 3. κ_{CCN} of **(a)** AS–dicarboxylic acid and **(b)** NaCl–dicarboxylic acid mixed particles with varied OVF.

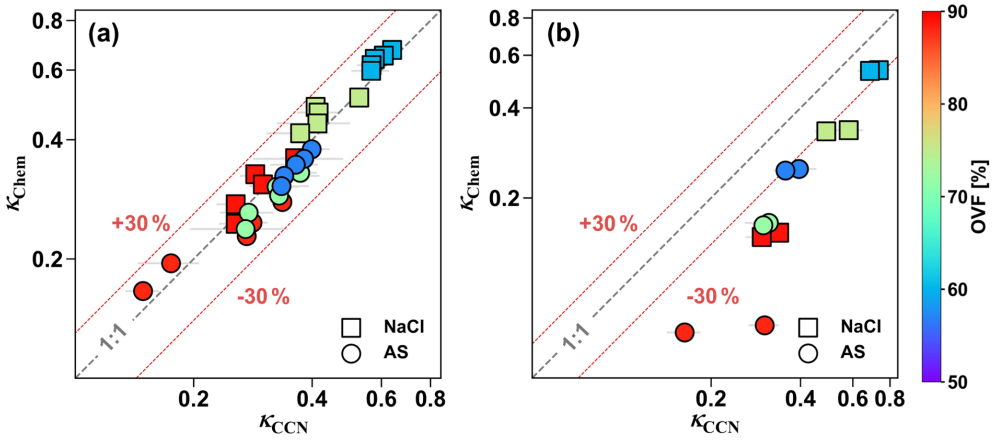

Figure 4. Comparison between κ_{CCN} and κ_{Chem} of **(a)** inorganic salt mixed with MA, PhMA, SA, PhSA, and PA and **(b)** inorganic salt mixed with AA and OA. Squares represent NaCl-containing particles, and circles represent AS-containing particles. The color bar indicates OVF.

and Tivanski, 2021). Figure 5a shows a force plot of mixed NaCl–MA particles with 75 % OVF. The AFM probe needle tip approached the droplet vertically before contact with the droplet, and the needle tip was not disturbed by extra force (red line). The needle tip then came into contact with the droplet, resulting in an abrupt negative force (i.e., the needle was attracted by the drop). After this the needle moved through the droplet with negative force until making contact with the substrate. When the tip made contact with the substrate, the negative force would quickly become positive (repulsive force), exceeding a predefined maximum amount of force. Following this, the tip retracted back away from the droplet, as indicated by the blue line. Because of the surface tension of droplet surface, the needle tip would experience attractive force and abruptly turn to zero when the tip separated from the droplet surface. Our observation in Fig. 5a showed a similar shape to the results reported by Morris et al. (2015), indicating that the particles were liquid. Most of the studied mixed inorganic salt and dicarboxylic acid (MA, PhMA, SA, PhSA and PA) particles were liquid under RH over 99.5 %.

However, for AS–SA (72 % and 88 % OVF), NaCl–AA (89 % OVF), AS–AA (57 %, 72 % and 88 % OVF), and AS–OA (88 % OVF) the shape force plots were totally different. As the tip made contact with the particle force plots showed a jagged profile, as shown in Fig. 5b. This shape is nearly the same as the curves for NaBr particles under 52 % RH reported by Lee et al. (2017a). They explained that the phase of NaBr was semi-solid and that the jagged profile as the tip approached was caused by its viscosity. Therefore, this indi-

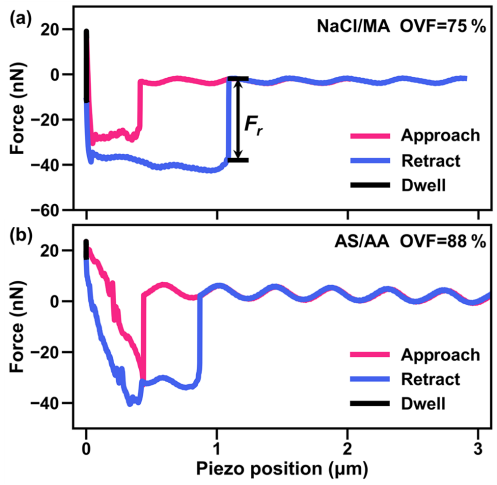

Figure 5. AFM force plots of **(a)** the NaCl–MA system with 75 % OVF and **(b)** the AS–AA system with 88 % OVF. F_r is the retention force to break the meniscus using the tip of the AFM probe.

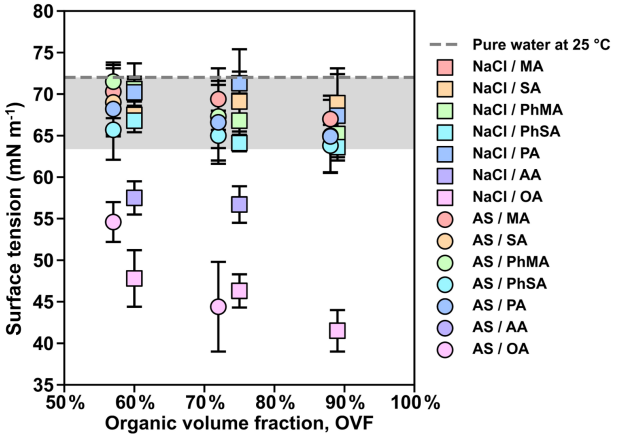

Figure 6. Measured surface tension values of inorganic salt and dicarboxylic acid particles under RH over 99.5 %. The gray area covers the surface tension reductions of below 12 % compared with pure water (72 mN m^{-1}).

cates that AS–SA (72 % and 88 % OVF), NaCl–AA (89 % OVF), AS–AA (57 %, 72 %, and 88 % OVF) and AS–OA (88 % OVF) mixed particles are semisolid. Semisolid phase states were more likely to occur when particles contained a higher OVF with dicarboxylic acids with lower solubilities and higher deliquescence points (SA, AA, and OA) and inorganic salts with comparative lower hygroscopicity (AS), as in this circumstance water content may be insufficient and could not easily dissolve organics. Therefore, the semisolid phase of mixed inorganic salt–AA and inorganic salt–OA particles provides evidence for a phase state effect on aerosol hygroscopicity, which may be attributable to higher κ_{CCN} than κ_{Chem}, as discussed in Sect. 3.3 (Fig. 4b). Though mixed AS–SA particles (72 % and 88 % OVF) were semisolid because of the high deliquescence point (98 %) of SA, their good closure between κ_{CCN} and κ_{Chem} may be ascribed to the higher solubility of SA, which may intensify the water absorption after deliquescence and thus the phase transition from semisolid to diluted liquid when activating to CCN.

3.4.2 Surface tension

Lee et al. (2017a) pointed out that surface tension calculation could not be achieved for semisolid particles because the measured retention force was not solely attributed to surface tension but also had additional contributions that include viscosity. Therefore, only surface tensions of mixed inorganic salt and dicarboxylic acid particles that were liquid were further obtained by Eq. (3). Surface tension results were summarized in Fig. 6. Overall, surface tensions of all mixed inorganic salt and dicarboxylic acid particles showed a decreasing trend with increased OVF, as higher OVF may result in higher organic solute concentrations and thus cause more surface tension reduction. Surface tensions of inorganic salts mixed with MA, PhMA, SA, PhSA, and PA were lower than that of pure water (72 mN m^{-1}) by within 12 %, indicating that droplets got strongly diluted at RH over 99.5 % and ought to be more diluted when activation occurs. This may contribute to κ closure within 30 % deviation in Fig. 4a because the diluted solution and water surface tension were assumed in κ-Köhler theory. However, surface tensions of inorganic salt–AA and inorganic salt–OA mixed particles showed notable reductions (20 %–42 %), which may contribute to their higher κ_{CCN} values than κ_{Chem} (Fig. 4b). Aside from this, notable surface tension reductions in particles containing OA or AA indicated that organic solubility plays an important role in surface tension reduction, as AA and OA have the lowest solubilities among studied dicarboxylic acids. OA and AA have higher carbon numbers than most of the other studied organics. Aumann et al. (2010) found that the surface activity of dicarboxylic acids increases with carbon number from 2 to 9 based on the surface tension measurement of their water solutions, indicating that dicarboxylic acids (e.g., OA and AA) with a higher carbon number have stronger surface activity. Therefore, the strong surface activity of dicarboxylic acid is another factor contributing to the surface tension reduction of inorganic salts and dicarboxylic acids. In order to quantitatively connect surface tension and measured κ_{CCN}, we used the solubility-involved Köhler model introduced by Petters and Kreidenweis (2008) to investigate the sensitivity of the measured κ_{CCN} values to the assumed value of surface tension for inorganic salt–OA systems. As shown in Fig. 7a, κ_{CCN} of NaCl–OA with 60 %, 75 %, and 89 % OVF derived from the solubility-involved Köhler model using water surface tension were 0.515, 0.324, and 0.145 (circles). These values underpredict measured κ_{CCN} (0.688, 0.485, and 0.296, triangles). However, if modeled κ_{CCN} values fit the measured values, the

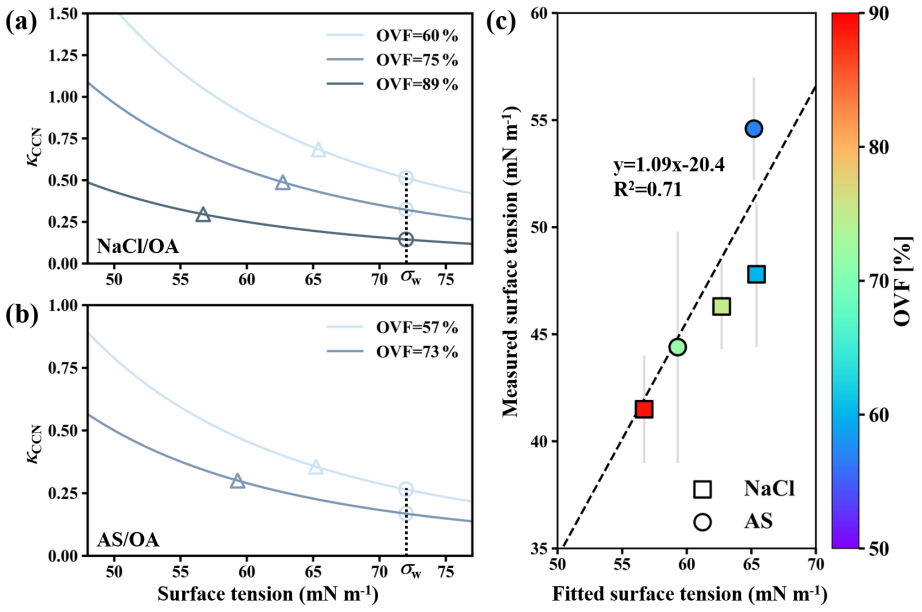

Figure 7. κ_{CCN} versus assumed surface tension for **(a)** NaCl–OA and **(b)** AS–OA systems according to solubility-involved Köhler model presented by Petters and Kreidenweis (2008). The triangles and circles in **(a)** and **(b)** represent the measured κ_{CCN} and predict κ_{CCN} by solubility-involved Köhler model. Closure between fitted surface tensions and measured surface tensions **(c)**. σ_w represents water surface tension (72 mN m^{-1}).

corresponding surface tension should reduce to 65.4 mN m^{-1} (60 % OVF), 62.7 mN m^{-1} (75 % OVF), and 56.7 mN m^{-1} (89 % OVF). Similar results were also found for AS–OA systems (Fig. 7b). In Fig. 7c, fitted surface tension showed good linear relations with measured surface tensions (slope and R^2 were 1.09 and 0.71). Therefore, our results could provide a quantitative way to predict κ_{CCN} values of inorganic salts and OA based on the solubility-involved Köhler model by using their measured surface tension results under high RH. This quantitative method should be tested for more chemical systems in the future.

4 Conclusions

The role of surfactants such as dicarboxylic acids in CCN activity has often been ignored in aerosol hygroscopicity studies and currently used climate models. In this study, we analyzed CCN activities of internally mixed inorganic salt–dicarboxylic acid particles with varied OVF and directly measured their phase state and surface tension using AFM under relatively high RH.

κ_{CCN} values of single dicarboxylic acids were located in the range of 0.003–0.240. A linearly positive correlation between κ_{CCN} and solubility was obtained for slightly dissolved species, while a negative correlation was found between κ_{CCN} and molecular volume for highly soluble species. κ_{CCN} of PhMA and PhSA were lower than those of MA and SA, respectively, revealing that addition of phenyl radical could weaken hygroscopicity of dicarboxylic acid.

For most inorganic salt–dicarboxylic acid (MA, PhMA, SA, PhSA and PA) combinations, κ_{CCN} of mixed particles with same OVF showed an overall decreasing trend and followed the order of κ_{CCN} values of single dicarboxylic acids. Good closure within 30 % relative bias between κ_{CCN} and κ_{Chem} was obtained. In contrast, our results demonstrate that the semisolid phase state and surface tension reduction (20 %–42 %) are potential factors to explain the enhanced CCN activity of inorganic salt–OA and inorganic salt–AA mixed particles. Dicarboxylic acids with lower solubilities and strong surface activity are more likely to cause notable surface tension depression for mixed inorganic salt–dicarboxylic acid particles. Therefore, we proposed that surface tension reduction and phase state should be carefully considered in future models and observations, especially for slightly soluble organics with strong surface activity.

Data availability. The data used in this paper can be obtained from the corresponding author upon request.

Supplement. The supplement related to this article is available online at: https://doi.org/10.5194/acp-22-16123-2022-supplement.

Author contributions. CX did the experiments, analyzed the data, plotted the figures, and wrote the original draft. BK contributed to data analysis and discussion, reviewed the manuscript, and contributed to funding acquisition. XC, XD, XP, and SY con-

tributed to the instrumentation and discussion. ZX contributed to the discussion and funding acquisition. HH contributed to the instrumentation, discussion, and funding acquisition. ZW administrated the project, conceptualized the study, reviewed the manuscript, and contributed to funding acquisition.

Competing interests. The contact author has declared that none of the authors has any competing interests.

Disclaimer. Publisher's note: Copernicus Publications remains neutral with regard to jurisdictional claims in published maps and institutional affiliations.

Acknowledgements. The research was supported by the National Natural Science Foundation of China (grant nos. 91844301, 42005087, 61974128 and 42005086) and the Fundamental Research Funds for the Central Universities (grant no. 2018QNA6008). We thank Lin Liu from the Instrumentation and Service Center for Physical Sciences at Westlake University for the supporting our AFM experiments. We likewise thank Changlong Liu, Ren Zhu, and Zhiwen Liu at Oxford Instruments; Renwei Mao at Zhejiang University; and Yuzhong Zhang at Westlake University for the discussions about AFM experiments.

Financial support. This research has been supported by the National Natural Science Foundation of China (grant nos. 91844301, 42005087, 61974128, and 42005086) and the Fundamental Research Funds for the Central Universities (grant no. 2018QNA6008).

Review statement. This paper was edited by Guangjie Zheng and reviewed by two anonymous referees.

References

Almeida, G. P., Brito, J., Morales, C. A., Andrade, M. F., and Artaxo, P.: Measured and modelled cloud condensation nuclei (CCN) concentration in São Paulo, Brazil: the importance of aerosol size-resolved chemical composition on CCN concentration prediction, Atmos. Chem. Phys., 14, 7559–7572, https://doi.org/10.5194/acp-14-7559-2014, 2014.

Asa-Awuku, A., Moore, R. H., Nenes, A., Bahreini, R., Holloway, J. S., Brock, C. A., Middlebrook, A. M., Ryerson, T. B., Jimenez, J. L., DeCarlo, P. F., Hecobian, A., Weber, R. J., Stickel, R., Tanner, D. J., and Huey, L. G.: Airborne cloud condensation nuclei measurements during the 2006 Texas Air Quality Study, J. Geophys. Res.-Atmos., 116, D11201, https://doi.org/10.1029/2010jd014874, 2011.

Aumann, E., Hildemann, L. M., and Tabazadeh, A.: Measuring and modeling the composition and temperature-dependence of surface tension for organic solutions, Atmos. Environ., 44, 329–337, https://doi.org/10.1016/j.atmosenv.2009.10.033, 2010.

Bhattu, D. and Tripathi, S. N.: CCN closure study: Effects of aerosol chemical composition and mixing state, J. Geophys. Res.-Atmos., 120, 766–783, https://doi.org/10.1002/2014jd021978, 2015.

Bilde, M. and Svenningsson, B.: CCN activation of slightly soluble organics: the importance of small amounts of inorganic salt and particle phase, Tellus B, 56, 128–134, https://doi.org/10.3402/tellusb.v56i2.16406, 2004.

Bzdek, B. R., Reid, J. P., Malila, J., and Prisle, N. L.: The surface tension of surfactant-containing, finite volume droplets, Proc. Natl. Acad. Sci. USA, 117, 8335–8343, https://doi.org/10.1073/pnas.1915660117, 2020.

Cai, M., Liang, B., Sun, Q., Zhou, S., Chen, X., Yuan, B., Shao, M., Tan, H., and Zhao, J.: Effects of continental emissions on cloud condensation nuclei (CCN) activity in the northern South China Sea during summertime 2018, Atmos. Chem. Phys., 20, 9153–9167, https://doi.org/10.5194/acp-20-9153-2020, 2020.

Chan, M. N., Kreidenweis, S. M., and Chan, C. K.: Measurements of the hygroscopic and deliquescence properties of organic compounds of different solubilities in water and their relationship with cloud condensation nuclei activities, Environ. Sci. Technol., 42, 3602–3608, https://doi.org/10.1021/es7023252, 2008.

Cheng, Y. F., Su, H., Koop, T., Mikhailov, E., and Poschl, U.: Size dependence of phase transitions in aerosol nanoparticles, Nat. Commun., 6, 1–7, https://doi.org/10.1038/ncomms6923, 2015.

Dawson, K. W., Petters, M. D., Meskhidze, N., Petters, S. S., and Kreidenweis, S. M.: Hygroscopic growth and cloud droplet activation of xanthan gum as a proxy for marine hydrogels, J. Geophys. Res.-Atmos., 121, 11803–11818, https://doi.org/10.1002/2016jd025143, 2016.

Ding, Q., Wang, J., Chen, X., Liu, H., Li, Q., Wang, Y., and Yang, S.: Quantitative and sensitive SERS platform with analyte enrichment and filtration function, Nano Lett., 20, 7304–7312, https://doi.org/10.1021/acs.nanolett.0c02683, 2020.

Ding, X., Kuang, B., Xiong, C., Mao, R., Xu, Y., Wang, Z., and Hu, H.: A Super High Aspect Ratio Atomic Force Microscopy Probe for Accurate Topography and Surface Tension Measurement, Sens. Actuators, A, 347, 113891, https://doi.org/10.1016/j.sna.2022.113891, 2022.

Dusek, U., Frank, G. P., Hildebrandt, L., Curtius, J., Schneider, J., Walter, S., Chand, D., Drewnick, F., Hings, S., Jung, D., Borrmann, S., and Andreae, M. O.: Size matters more than chemistry for cloud-nucleating ability of aerosol particles, Science, 312, 1375–1378, https://doi.org/10.1126/science.1125261, 2006.

Facchini, M. C., Mircea, M., Fuzzi, S., and Charlson, R. J.: Cloud albedo enhancement by surface-active organic solutes in growing droplets, Nature, 401, 257–259, https://doi.org/10.1038/45758, 1999.

Gerard, V., Noziere, B., Baduel, C., Fine, L., Frossard, A. A., and Cohen, R. C.: Anionic, Cationic, and Nonionic Surfactants in Atmospheric Aerosols from the Baltic Coast at Asko, Sweden: Implications for Cloud Droplet Activation, Environ. Sci. Technol., 50, 2974–2982, https://doi.org/10.1021/acs.est.5b05809, 2016.

Good, N., Topping, D. O., Allan, J. D., Flynn, M., Fuentes, E., Irwin, M., Williams, P. I., Coe, H., and McFiggans, G.: Consistency between parameterisations of aerosol hygroscopicity and CCN activity during the RHaMBLe discovery cruise, Atmos. Chem. Phys., 10, 3189–3203, https://doi.org/10.5194/acp-10-3189-2010, 2010.

Gunthe, S. S., King, S. M., Rose, D., Chen, Q., Roldin, P., Farmer, D. K., Jimenez, J. L., Artaxo, P., Andreae, M. O., Martin, S. T., and Pöschl, U.: Cloud condensation nuclei in pristine tropical rainforest air of Amazonia: size-resolved measurements and modeling of atmospheric aerosol composition and CCN activity, Atmos. Chem. Phys., 9, 7551–7575, https://doi.org/10.5194/acp-9-7551-2009, 2009.

Han, S., Hong, J., Luo, Q., Xu, H., Tan, H., Wang, Q., Tao, J., Zhou, Y., Peng, L., He, Y., Shi, J., Ma, N., Cheng, Y., and Su, H.: Hygroscopicity of organic compounds as a function of organic functionality, water solubility, molecular weight, and oxidation level, Atmos. Chem. Phys., 22, 3985–4004, https://doi.org/10.5194/acp-22-3985-2022, 2022.

Henning, S., Rosenørn, T., D'Anna, B., Gola, A. A., Svenningsson, B., and Bilde, M.: Cloud droplet activation and surface tension of mixtures of slightly soluble organics and inorganic salt, Atmos. Chem. Phys., 5, 575–582, https://doi.org/10.5194/acp-5-575-2005, 2005.

Hings, S. S., Wrobel, W. C., Cross, E. S., Worsnop, D. R., Davidovits, P., and Onasch, T. B.: CCN activation experiments with adipic acid: effect of particle phase and adipic acid coatings on soluble and insoluble particles, Atmos. Chem. Phys., 8, 3735–3748, https://doi.org/10.5194/acp-8-3735-2008, 2008.

Ho, K. F., Lee, S. C., Ho, S. S. H., Kawamura, K., Tachibana, E., Cheng, Y., and Zhu, T.: Dicarboxylic acids, ketocarboxylic acids, α-dicarbonyls, fatty acids, and benzoic acid in urban aerosols collected during the 2006 Campaign of Air Quality Research in Beijing (CAREBeijing-2006), J. Geophys. Res.-Atmos., 115, D19312, https://doi.org/10.1029/2009jd013304, 2010.

Hodas, N., Zuend, A., Mui, W., Flagan, R. C., and Seinfeld, J. H.: Influence of particle-phase state on the hygroscopic behavior of mixed organic–inorganic aerosols, Atmos. Chem. Phys., 15, 5027–5045, https://doi.org/10.5194/acp-15-5027-2015, 2015.

Hu, D., Liu, D., Zhao, D., Yu, C., Liu, Q., Tian, P., Bi, K., Ding, S., Hu, K., Wang, F., Wu, Y., Wu, Y., Kong, S., Zhou, W., He, H., Huang, M., and Ding, D.: Closure investigation on cloud condensation nuclei ability of processed anthropogenic aerosols, J. Geophys. Res.-Atmos., 125, e2020JD032680, https://doi.org/10.1029/2020jd032680, 2020.

Hyder, M., Genberg, J., Sandahl, M., Swietlicki, E., and Jönsson, J. Å.: Yearly trend of dicarboxylic acids in organic aerosols from south of Sweden and source attribution, Atmos. Environ., 57, 197–204, https://doi.org/10.1016/j.atmosenv.2012.04.027, 2012.

Irwin, M., Good, N., Crosier, J., Choularton, T. W., and McFiggans, G.: Reconciliation of measurements of hygroscopic growth and critical supersaturation of aerosol particles in central Germany, Atmos. Chem. Phys., 10, 11737–11752, https://doi.org/10.5194/acp-10-11737-2010, 2010.

Jurányi, Z., Gysel, M., Weingartner, E., DeCarlo, P. F., Kammermann, L., and Baltensperger, U.: Measured and modelled cloud condensation nuclei number concentration at the high alpine site Jungfraujoch, Atmos. Chem. Phys., 10, 7891–7906, https://doi.org/10.5194/acp-10-7891-2010, 2010.

Kaluarachchi, C. P., Lee, H. D., Lan, Y., Lansakara, T. I., and Tivanski, A. V.: Surface tension measurements of aqueous liquid-air interfaces probed with microscopic indentation, Langmuir, 37, 2457–2465, https://doi.org/10.1021/acs.langmuir.0c03507, 2021.

Kawana, K., Nakayama, T., and Mochida, M.: Hygroscopicity and CCN activity of atmospheric aerosol particles and their relation to organics: Characteristics of urban aerosols in Nagoya, Japan, J. Geophys. Res.-Atmos., 121, 4100–4121, https://doi.org/10.1002/2015jd023213, 2016.

Köhler, H.: The nucleus in and the growth of hygroscopic droplets, Trans. Faraday Soc., 32, 1152–1161, https://doi.org/10.1039/tf9363201152, 1936.

Kuwata, M., Shao, W., Lebouteiller, R., and Martin, S. T.: Classifying organic materials by oxygen-to-carbon elemental ratio to predict the activation regime of Cloud Condensation Nuclei (CCN), Atmos. Chem. Phys., 13, 5309–5324, https://doi.org/10.5194/acp-13-5309-2013, 2013.

Lee, H. D., Estillore, A. D., Morris, H. S., Ray, K. K., Alejandro, A., Grassian, V. H., and Tivanski, A. V.: Direct surface tension measurements of individual sub-micrometer particles using atomic force microscopy, J. Phys. Chem. A, 121, 8296–8305, https://doi.org/10.1021/acs.jpca.7b04041, 2017a.

Lee, H. D., Ray, K. K., and Tivanski, A. V.: Solid, semisolid, and liquid phase states of individual submicrometer particles directly probed using atomic force microscopy, Anal. Chem., 89, 12720–12726, https://doi.org/10.1021/acs.analchem.7b02755, 2017b.

Lee, H. D., Morris, H. S., Laskina, O., Sultana, C. M., Lee, C., Jayarathne, T., Cox, J. L., Wang, X., Hasenecz, E. S., DeMott, P. J., Bertram, T. H., Cappa, C. D., Stone, E. A., Prather, K. A., Grassian, V. H., and Tivanski, A. V.: Organic enrichment, physical phase state, and surface tension depression of nascent core–shell sea spray aerosols during two phytoplankton blooms, ACS Earth Space Chem., 4, 650–660, https://doi.org/10.1021/acsearthspacechem.0c00032, 2020.

Lee, H. D. and Tivanski, A. V.: Atomic force microscopy: An emerging tool in measuring the phase state and surface tension of individual aerosol particles, Annu. Rev. Phys. Chem., 72, 235–252, https://doi.org/10.1146/annurev-physchem-090419-110133, 2021.

Lee, J. Y. and Hildemann, L. M.: Surface tension of solutions containing dicarboxylic acids with ammonium sulfate, d-glucose, or humic acid, J. Aerosol Sci., 64, 94–102, https://doi.org/10.1016/j.jaerosci.2013.06.004, 2013.

Lee, J. Y. and Hildemann, L. M.: Surface tensions of solutions containing dicarboxylic acid mixtures, Atmos. Environ., 89, 260–267, https://doi.org/10.1016/j.atmosenv.2014.02.049, 2014.

Liu, P. F., Song, M. J., Zhao, T. N., Gunthe, S. S., Ham, S. H., He, Y. P., Qin, Y. M., Gong, Z. H., Amorim, J. C., Bertram, A. K., and Martin, S. T.: Resolving the mechanisms of hygroscopic growth and cloud condensation nuclei activity for organic particulate matter, Nat. Commun., 9, 4076, https://doi.org/10.1038/s41467-018-06622-2, 2018.

Lowe, S. J., Partridge, D. G., Davies, J. F., Wilson, K. R., Topping, D., and Riipinen, I.: Key drivers of cloud response to surface-active organics, Nat. Commun., 10, 5214, https://doi.org/10.1038/s41467-019-12982-0, 2019.

Luo, Q. W., Hong, J., Xu, H. B., Han, S., Tan, H. B., Wang, Q. Q., Tao, J. C., Ma, N., Cheng, Y. F., and Su, H.: Hygroscopicity of amino acids and their effect on the water uptake of ammonium sulfate in the mixed aerosol particles, Sci. Total Environ., 734, 139318, https://doi.org/10.1016/j.scitotenv.2020.139318, 2020.

Metcalf, A. R., Boyer, H. C., and Dutcher, C. S.: Interfacial tensions of aged organic aerosol particle mimics using a biphasic

microfluidic platform, Environ. Sci. Technol., 50, 1251–1259, https://doi.org/10.1021/acs.est.5b04880, 2016.

Minambres, L., Mendez, E., Sanchez, M. N., Castano, F., and Basterretxea, F. J.: Water uptake of internally mixed ammonium sulfate and dicarboxylic acid particles probed by infrared spectroscopy, Atmos. Environ., 70, 108–116, https://doi.org/10.1016/j.atmosenv.2013.01.007, 2013.

Moore, R. H. and Nenes, A.: Scanning Flow CCN Analysis – A Method for Fast Measurements of CCN Spectra, Aerosol Sci. Technol., 43, 1192–1207, https://doi.org/10.1080/02786820903289780, 2009.

Morris, H. S., Grassian, V. H., and Tivanski, A. V.: Humidity-dependent surface tension measurements of individual inorganic and organic submicrometre liquid particles, Chem. Sci., 6, 3242–3247, https://doi.org/10.1039/c4sc03716b, 2015.

Nguyen, Q. T., Kjær, K. H., Kling, K. I., Boesen, T., and Bilde, M.: Impact of fatty acid coating on the CCN activity of sea salt particles, Tellus B, 69, 1304064, https://doi.org/10.1080/16000889.2017.1304064, 2017.

Noziere, B.: Don't forget the surface, Science, 351, 1396–1397, https://doi.org/10.1126/science.aaf3253, 2016.

Ovadnevaite, J., Zuend, A., Laaksonen, A., Sanchez, K. J., Roberts, G., Ceburnis, D., Decesari, S., Rinaldi, M., Hodas, N., Facchini, M. C., Seinfeld, J. H., and O'Dowd, C.: Surface tension prevails over solute effect in organic-influenced cloud droplet activation, Nature, 546, 637–641, https://doi.org/10.1038/nature22806, 2017.

Pajunoja, A., Lambe, A. T., Hakala, J., Rastak, N., Cummings, M. J., Brogan, J. F., Hao, L. Q., Paramonov, M., Hong, J., Prisle, N. L., Malila, J., Romakkaniemi, S., Lehtinen, K. E. J., Laaksonen, A., Kulmala, M., Massoli, P., Onasch, T. B., Donahue, N. M., Riipinen, I., Davidovits, P., Worsnop, D. R., Petaja, T., and Virtanen, A.: Adsorptive uptake of water by semisolid secondary organic aerosols, Geophys. Res. Lett., 42, 3063–3068, https://doi.org/10.1002/2015gl063142, 2015.

Parsons, M. T., Mak, J., Lipetz, S. R., and Bertram, A. K.: Deliquescence of malonic, succinic, glutaric, and adipic acid particles, J. Geophys. Res.-Atmos., 109, D06212, https://doi.org/10.1029/2003jd004075, 2004.

Peng, C., Chan, M. N., and Chan, C. K.: The hygroscopic properties of dicarboxylic and multifunctional acids: Measurements and UNIFAC predictions, Environ. Sci. Technol., 35, 4495–4501, https://doi.org/10.1021/es0107531, 2001.

Peng, C., Jing, B., Guo, Y. C., Zhang, Y. H., and Ge, M. F.: Hygroscopic behavior of multicomponent aerosols involving NaCl and dicarboxylic Acids, J. Phys. Chem. A, 120, 1029–1038, https://doi.org/10.1021/acs.jpca.5b09373, 2016.

Peng, C., Razafindrambinina, P. N., Malek, K. A., Chen, L., Wang, W., Huang, R.-J., Zhang, Y., Ding, X., Ge, M., Wang, X., Asa-Awuku, A. A., and Tang, M.: Interactions of organosulfates with water vapor under sub- and supersaturated conditions, Atmos. Chem. Phys., 21, 7135–7148, https://doi.org/10.5194/acp-21-7135-2021, 2021.

Peng, C., Chen, L., and Tang, M.: A database for deliquescence and efflorescence relative humidities of compounds with atmospheric relevance, Fundam. Res., 2, 578–587, https://doi.org/10.1016/j.fmre.2021.11.021, 2022.

Petters, M. D. and Kreidenweis, S. M.: A single parameter representation of hygroscopic growth and cloud condensation nucleus activity, Atmos. Chem. Phys., 7, 1961–1971, https://doi.org/10.5194/acp-7-1961-2007, 2007.

Petters, M. D. and Kreidenweis, S. M.: A single parameter representation of hygroscopic growth and cloud condensation nucleus activity – Part 2: Including solubility, Atmos. Chem. Phys., 8, 6273–6279, https://doi.org/10.5194/acp-8-6273-2008, 2008.

Petters, M. D., Kreidenweis, S. M., Prenni, A. J., Sullivan, R. C., Carrico, C. M., Koehler, K. A., and Ziemann, P. J.: Role of molecular size in cloud droplet activation, Geophys. Res. Lett., 36, L22801, https://doi.org/10.1029/2009gl040131, 2009.

Petters, S. S., Pagonis, D., Claflin, M. S., Levin, E. J. T., Petters, M. D., Ziemann, P. J., and Kreidenweis, S. M.: Hygroscopicity of organic compounds as a function of carbon chain length and carboxyl, hydroperoxy, and carbonyl functional groups, J. Phys. Chem. A, 121, 5164–5174, https://doi.org/10.1021/acs.jpca.7b04114, 2017.

Pradeep Kumar, P., Broekhuizen, K., and Abbatt, J. P. D.: Organic acids as cloud condensation nuclei: Laboratory studies of highly soluble and insoluble species, Atmos. Chem. Phys., 3, 509–520, https://doi.org/10.5194/acp-3-509-2003, 2003.

Ray, K. K., Lee, H. D., Gutierrez, M. A., Jr., Chang, F. J., and Tivanski, A. V.: Correlating 3D morphology, phase state, and viscoelastic properties of individual substrate-deposited particles, Anal. Chem., 91, 7621–7630, https://doi.org/10.1021/acs.analchem.9b00333, 2019.

Römpp, A., Winterhalter, R., and Moortgat, G. K.: Oxodicarboxylic acids in atmospheric aerosol particles, Atmos. Environ., 40, 6846–6862, https://doi.org/10.1016/j.atmosenv.2006.05.053, 2006.

Rose, D., Gunthe, S. S., Mikhailov, E., Frank, G. P., Dusek, U., Andreae, M. O., and Pöschl, U.: Calibration and measurement uncertainties of a continuous-flow cloud condensation nuclei counter (DMT-CCNC): CCN activation of ammonium sulfate and sodium chloride aerosol particles in theory and experiment, Atmos. Chem. Phys., 8, 1153–1179, https://doi.org/10.5194/acp-8-1153-2008, 2008.

Rose, D., Nowak, A., Achtert, P., Wiedensohler, A., Hu, M., Shao, M., Zhang, Y., Andreae, M. O., and Pöschl, U.: Cloud condensation nuclei in polluted air and biomass burning smoke near the mega-city Guangzhou, China – Part 1: Size-resolved measurements and implications for the modeling of aerosol particle hygroscopicity and CCN activity, Atmos. Chem. Phys., 10, 3365–3383, https://doi.org/10.5194/acp-10-3365-2010, 2010.

Rosenfeld, D., Sherwood, S., Wood, R., and Donner, L.: Climate effects of aerosol–cloud interactions, Science, 343, 379–380, https://doi.org/10.1126/science.1247490, 2014.

Ruehl, C. R. and Wilson, K. R.: Surface organic monolayers control the hygroscopic growth of submicrometer particles at high relative humidity, J. Phys. Chem. A, 118, 3952–3966, https://doi.org/10.1021/jp502844g, 2014.

Ruehl, C. R., Chuang, P. Y., and Nenes, A.: Aerosol hygroscopicity at high (99 to 100 %) relative humidities, Atmos. Chem. Phys., 10, 1329–1344, https://doi.org/10.5194/acp-10-1329-2010, 2010.

Ruehl, C. R., Chuang, P. Y., Nenes, A., Cappa, C. D., Kolesar, K. R., and Goldstein, A. H.: Strong evidence of surface tension reduction in microscopic aqueous droplets, Geophys. Res. Lett., 39, L23801, https://doi.org/10.1029/2012gl053706, 2012.

Ruehl, C. R., Davies, J. F., and Wilson, K. R.: An interfacial mechanism for cloud droplet formation on organic aerosols, Science, 351, 1447–1450, https://doi.org/10.1126/science.aad4889, 2016.

Shiraiwa, M., Li, Y., Tsimpidi, A. P., Karydis, V. A., Berkemeier, T., Pandis, S. N., Lelieveld, J., Koop, T., and Poschl, U.: Global distribution of particle phase state in atmospheric secondary organic aerosols, Nat. Commun., 8, 15002, https://doi.org/10.1038/ncomms15002, 2017.

Sjogren, S., Gysel, M., Weingartner, E., Baltensperger, U., Cubison, M. J., Coe, H., Zardini, A. A., Marcolli, C., Krieger, U. K., and Peter, T.: Hygroscopic growth and water uptake kinetics of two-phase aerosol particles consisting of ammonium sulfate, adipic and humic acid mixtures, J. Aerosol Sci., 38, 157–171, https://doi.org/10.1016/j.jaerosci.2006.11.005, 2007.

Suda, S. R., Petters, M. D., Yeh, G. K., Strollo, C., Matsunaga, A., Faulhaber, A., Ziemann, P. J., Prenni, A. J., Carrico, C. M., Sullivan, R. C., and Kreidenweis, S. M.: Influence of functional groups on organic aerosol cloud condensation nucleus activity, Environ. Sci. Technol., 48, 10182–10190, https://doi.org/10.1021/es502147y, 2014.

Vepsäläinen, S., Calderón, S. M., Malila, J., and Prisle, N. L.: Comparison of six approaches to predicting droplet activation of surface active aerosol – Part 1: moderately surface active organics, Atmos. Chem. Phys., 22, 2669–2687, https://doi.org/10.5194/acp-22-2669-2022, 2022.

Wu, Z. J., Poulain, L., Henning, S., Dieckmann, K., Birmili, W., Merkel, M., van Pinxteren, D., Spindler, G., Müller, K., Stratmann, F., Herrmann, H., and Wiedensohler, A.: Relating particle hygroscopicity and CCN activity to chemical composition during the HCCT-2010 field campaign, Atmos. Chem. Phys., 13, 7983–7996, https://doi.org/10.5194/acp-13-7983-2013, 2013.

Yazdanpanah, M. M., Hosseini, M., Pabba, S., Berry, S. M., Dobrokhotov, V. V., Safir, A., Keynton, R. S., and Cohn, R. W.: Micro-wilhelmy and related liquid property measurements using constant-diameter nanoneedle-tipped atomic force microscope probes, Langmuir, 24, 13753–13764, https://doi.org/10.1021/la802820u, 2008.

Zhang, C., Bu, L., Fan, F., Ma, N., Wang, Y., Yang, Y., Größ, J., Yan, J., and Wiedensohler, A.: Surfactant effect on the hygroscopicity of aerosol particles at relative humidity ranging from 80 % to 99.5 %: Internally mixed adipic acid-ammonium sulfate particles, Atmos. Environ., 266, 118725–118736, https://doi.org/10.1016/j.atmosenv.2021.118725, 2021.

Zhang, H., Xie, C., Liu, Z. K., Gong, J. B., Bao, Y., Zhang, M. J., Hao, H. X., Hou, B. H., and Yin, Q. X.: Identification and Molecular Understanding of the Odd-Even Effect of Dicarboxylic Acids Aqueous Solubility, Ind. Eng. Chem. Res., 52, 18458–18465, https://doi.org/10.1021/ie4030837, 2013.

Zhang, Y., Tao, J., Ma, N., Kuang, Y., Wang, Z., Cheng, P., Xu, W., Yang, W., Zhang, S., Xiong, C., Dong, W., Xie, L., Sun, Y., Fu, P., Zhou, G., Cheng, Y., and Su, H.: Predicting cloud condensation nuclei number concentration based on conventional measurements of aerosol properties in the North China Plain, Sci. Total Environ., 719, 137473, https://doi.org/10.1016/j.scitotenv.2020.137473, 2020.

Zhao, D. F., Buchholz, A., Kortner, B., Schlag, P., Rubach, F., Fuchs, H., Kiendler-Scharr, A., Tillmann, R., Wahner, A., Watne, Å. K., Hallquist, M., Flores, J. M., Rudich, Y., Kristensen, K., Hansen, A. M. K., Glasius, M., Kourtchev, I., Kalberer, M., and Mentel, Th. F.: Cloud condensation nuclei activity, droplet growth kinetics, and hygroscopicity of biogenic and anthropogenic secondary organic aerosol (SOA), Atmos. Chem. Phys., 16, 1105–1121, https://doi.org/10.5194/acp-16-1105-2016, 2016.